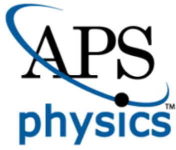

CHORUS

This is the accepted manuscript made available via CHORUS. The article has been published as:

Reducing orbital occupancy in VO_{2} suppresses Mott physics while Peierls distortions persist

Nicholas F. Quackenbush, Hanjong Paik, Megan E. Holtz, Matthew J. Wahila, Jarrett A. Moyer, Stefan Barthel, Tim O. Wehling, Dario A. Arena, Joseph C. Woicik, David A. Muller, Darrell G. Schlom, and Louis F. J. Piper

Phys. Rev. B **96**, 081103 — Published 8 August 2017

DOI: 10.1103/PhysRevB.96.081103

Reducing orbital occupancy in VO_2 suppresses Mott physics while Peierls distortions persist

Nicholas F. Quackenbush,[1,2] Hanjong Paik,[3] Megan E. Holtz,[4,5] Matthew J. Wahila,[1] Jarrett A. Moyer,[6] Stefan Barthel,[7,8] Tim Wehling,[7,8] Dario A. Arena,[9] Joseph C. Woicik,[10] David A. Muller,[4,5] Darrell G. Schlom,[3,5] and Louis F. J. Piper[1,11,*]

[1]*Department of Physics, Applied Physics and Astronomy, Binghamton University, Binghamton, New York 13902, USA*
[2]*Materials Measurement Science Division, National Institute of Standards and Technology, Gaithersburg, Maryland 20899, USA*
[3]*Department of Materials Science and Engineering, Cornell University, Ithaca, New York 14853-1501, USA*
[4]*School of Applied and Engineering Physics, Cornell University, Ithaca, NY 14853, USA*
[5]*Kavli Institute at Cornell for Nanoscale Science, Ithaca, New York 14853, USA*
[6]*Department of Physics and Materials Research Laboratory, University of Illinois at Urbana-Champaign, Urbana, IL 61801, USA*
[7]*Institut für Theoretische Physik, Universität Bremen, Otto-Hahn-Allee 1, 28359 Bremen, Germany*
[8]*Bremen Center for Computational Materials Science, Universitat Bremen, Am Fallturm 1a, 28359 Bremen, Germany*
[9]*Department of Physics, University of South Florida, Tampa, FL 33620*
[10]*Materials Science and Engineering Laboratory, National Institute of Standards and Technology, Gaithersburg, Maryland 20899, USA*
[11]*Materials Science & Engineering, Binghamton University, Binghamton, New York 13902, USA*

The characteristics of the cooperative Mott-Peierls metal-insulator transition (MIT) of VO_2 can be altered by employing epitaxial strain. While, the most commonly used substrate for this purpose is isostructural rutile TiO_2, thin films often suffer from interdiffusion of Ti ions near the interface. Exploiting this phenomena, we investigate the nature of interfacial V^{4+}/Ti^{4+} cation intermixing and its effects on the MIT using scanning transmission electron microscopy with electron energy loss spectroscopy (STEM-EELS), soft x-ray absorption spectroscopy (XAS), and hard x-ray photoelectron spectroscopy (HAXPES), along with supporting density functional theory (DFT) calculations. We find that the reduced orbital occupancy in highly Ti incorporated VO_2 is responsible for suppressing the MIT. Interdiffused films are found to be metallic at all measured temperatures, despite a resolute dimerization inferred from x-ray absorption data at lower temperatures. Our results demonstrate that the Mott physics can be suppressed in doped VO_2, while a lattice dimerization remains thermodynamically favorable.

Correlated oxides that undergo abrupt phase transitions, such as vanadium dioxide (VO_2), show great promise for use in advanced oxide electronics. VO_2 exhibits a cooperative Mott-Peierls metal-insulator transition (MIT) that is accompanied by a structural phase transition (SPT) from the tetragonal rutile structure to the lower symmetry monoclinic M1 structure.[1–3] The collective interactions that govern this MIT lead to ultrafast bulk switching, offering some key advantages over traditional oxide semiconductors.[4] For example, employing VO_2 as the active layer in a three terminal field effect transistor (FET) circumvents conventional restrictions such as 'Thomas-Fermi screening' and the 'Boltzmann limit', enabling ultra-thin and high-efficiency FETs.[5,6] More broadly, this MIT can be triggered by thermal, electrical, or optical means, which makes it practical for a wide range of switching devices.[7–9]

A promising route toward tuning the functionality of VO_2 is modifying the exact orbital occupancy within the valence V $3d$ band.[10] Recent progress in this effort has shown that the occupation of the so called $d_{\parallel}$ ($d_{x^2-y^2}$) orbital can be preferentially increased to foster a more purely Mott transition via strain.[11] In the other direction, decreasing the orbital occupancy of this $d_{\parallel}$ orbital could potentially be achieved by the introduction of certain dopants. For example, from a purely chemical standpoint, substituting a portion of V^{4+} (d^1) ions with Ti^{4+} (d^0) ions should introduce holes and thus reduce the overall orbital occupancy in the V $3d$ band. In fact, interdiffusion of Ti ions from commonly used rutile TiO_2 substrates has been known to occur during growth of VO_2 films, but has thus far only been considered as a detriment to the MIT and the intrinsic properties have not been thoroughly studied.[12–17]

Starting with VO_2/TiO_2 films with near atomically sharp interfaces, in this Rapid Communication we controllably introduce Ti interdiffusion to study its effect on the orbital occupancy of VO_2. We determine Ti-incorporated VO_2 films to display no evidence of an electronic MIT, exhibiting the low resistivity characteristic of metallic VO_2 at all temperatures. However, these films maintain a Peierls-like structural distortion, exhibiting a room temperature metallic phase with V-V dimerization. This suppression of the MIT, despite the persistent structural change, is explained within a hole doping model using Density Functional Theory (DFT) for both rutile and monoclinic VO_2. These results offer valuable insight into the longstanding issue of determining the precise rela-

tionship between the electronic MIT and accompanying SPT in VO_2.

A set of epitaxial VO_2 films that display abrupt changes in resistivity of a few orders of magnitude were grown on $TiO_2(100)$ substrates to thicknesses of 1-7.5 nm by reactive molecular beam epitaxy (MBE).[17–19] To achieve high quality interfaces, substrates were prepared by etching and annealing to have clean and well-defined atomic step and terrace microstructured surfaces.[20] After the initial growth, samples were thermally stressed to promote V/Ti cation intermixing. The onset of significant diffusion at the interface was found at a relatively mild temperature of 350 °C. We focus on a 7.5 nm film annealed in vacuum to 350 °C for 2 hours where an O_2 partial pressure of 1.3×10^{-6} mbar was used to suppress the formation of oxygen vacancies and reduction of vanadium to a 3^+ oxidation state.

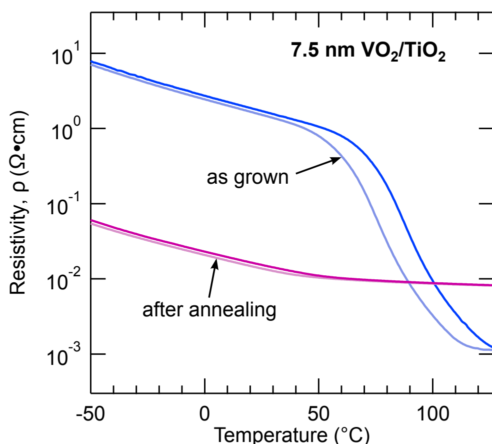

FIG. 1. The temperature-dependent resistivity of the same 7.5 nm VO_2/TiO_2 film before and after interfacial diffusion has occurred.

The temperature-dependent resistivity measurements of the film before and after interfacial diffusion was induced is shown in Fig. 1. The as-grown VO_2/TiO_2 film displays a transition with T_{MIT} centered at 84.8 °C, a change in resistivity of $\Delta R/R = 10^{3.0}$, and a hysteresis of 11.8 °C. Post-annealing, the film displays no sharp discontinuity in resistivity. The MIT, is entirely suppressed leaving the film in a low resistivity state at all measured temperatures. We note that the resistivity of the interdiffused film is higher than the original metallic state, as seen in Fig. 1, which is likely a consequence of the inhomogeneous concentration of Ti ions and resulting charge distribution.

Scanning transmission electron microscopy with electron energy loss spectroscopy (STEM-EELS) was employed to investigate the extent of interdiffusion in the region of the interface. Figure 2a and f show cross-sectional annular dark field (ADF) STEM images collected from the 7.5 nm VO_2/TiO_2 film before and after annealing, respectively. Uniform structure is observed in the as-grown film with no obvious sign of defects. The undamaged thickness of the film is 6.9–7.0 nm, while the top surface layer shows damage from ion milling during sample preparation. After annealing, the film appeared to have additional roughening of the surface and small regions of a possible second phase (indicated by the yellow arrow), although the majority of the film retained its structure.

The close proximity in atomic number of vanadium and titanium results in poor contrast between the VO_2 film and TiO_2 substrate in ADF imaging, however the spectroscopic images of vanadium and titanium reveal a sharp well-ordered interface before annealing (Fig. 2b-d) and an extremely diffuse interface afterwards (Fig. 2g-i). Before annealing, the vanadium has a uniform intensity throughout the film and the titanium is confined to the substrate and has not diffused into the film. After annealing, the titanium is present throughout the 7.5 nm film and appears in Fig. 2i to be sitting substitutionally on the vanadium sites. In the annealed film in Fig. 2h, the vanadium appears blurrier than in the as-grown case due to imperfect background subtraction from the titanium in the film and does not indicate disorder of the vanadium atoms.

Vertical line profiles of the vanadium and titanium concentrations are shown in Fig. 2e and j. Before annealing the line profiles show a sharp interface between titanium and vanadium with less than 1 nm of interdiffusion. After annealing, the titanium had a decaying concentration in the film, with significant quantities of titanium extending to the top of the film.

To probe the titanium environment within the VO_2 film, we use x-ray spectroscopy. Figure 3 shows the soft x-ray absorption spectroscopy (XAS) of the Ti L- and V L-edges measured at room temperature. The XAS was measured in total electron yield (TEY) mode and is therefore only sensitive to within the top few nanometers of the film.[19] For comparison, a reference 5 nm thick VO_2/TiO_2 film shows no Ti L-edge signal at all from the underlying substrate (Fig. 3a). This demonstrates that the lineshapes observed for the 7.5 nm interdiffused film is exclusively probing the Ti ions that have migrated into the film. The Ti L-edge is sensitive to oxidation state, local coordination, and symmetry around the Ti atom. Comparing this Ti L-edge spectrum to that of a TiO_2 single crystal, the lineshapes are nearly identical. This indicates the diffused Ti ions retain their 4^+ oxidation state and similar coordination environments within the VO_2 film. There is however a subtle modification of the feature at ∼460 eV, which can be attributed to differences in the next nearest Ti environments between the interdiffused and reference films.

Figure 3b shows the V L-edge, sampling the same depth of the two films. The XAS was measured with the linear polarization (E) of the incident x-ray beam aligned either parallel or perpendicular to the c_R axis of the VO_2 film. The similar lineshapes indicate no vanadium reduction or oxidation from its 4^+ valence has occurred. The reference film displays a strong dichroism, commonly observed as a signature of the highly directional monoclinic phase of VO_2.[21] The interdiffused film displays a similar

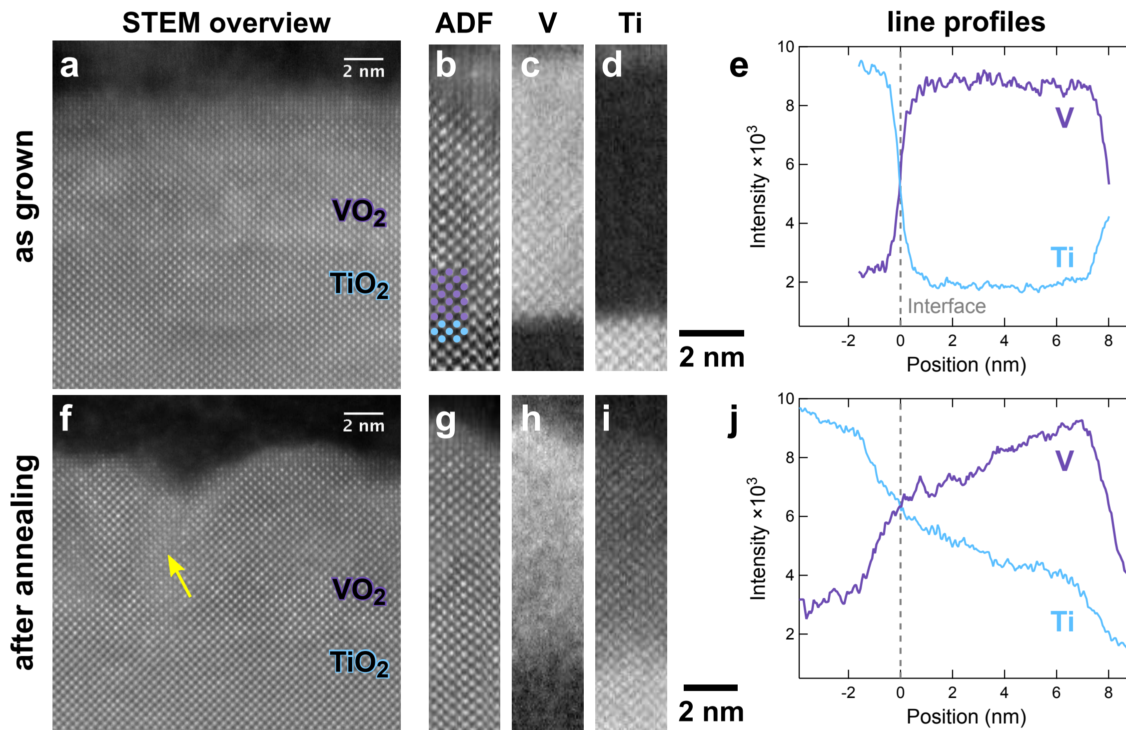

FIG. 2. Scanning transmission electron microscopy and electron energy-loss spectroscopy of $VO_2/TiO_2(100)$ films before and after annealing. (a) Overview image of the as-grown film. Simultaneous (b) annular dark field image, (c) vanadium, and (d) titanium spectroscopic images of the as-grown film. (e) Line profile of the vanadium and titanium concentrations showing a sharp interface for the as-grown film. (f) Overview image of the annealed film. Simultaneous (g) annular dark field image, (h) vanadium, and (i) titanium spectroscopic images of the annealed film. (j) Line profile of the vanadium and titanium concentrations showing a diffuse interface for the annealed film. All data is recorded in projection along the [001] axis.

slightly weaker dichroism, suggesting that the local structure around the vanadium has not significantly changed from the monoclinic structure, despite the incorporation of titanium ions. Additionally, further confirmation of both the Ti^{4+} and V^{4+} oxidation states was provided by our EELS and core level hard x-ray photoelectron spectroscopy (HAXPES) measurements (see supplemental material[22]).

The temperature dependent behavior of the interdiffused film was investigated by valence band HAXPES and O K-edge XAS. Figure 4a shows the topmost valence states measured at 23 °C (below T_{MIT}) and 120 °C (above T_{MIT}) for both the interdiffused film and reference film using a photon energy of 4 keV. The topmost states are mainly V 3d in character and display a large transfer of spectral weight near the Fermi level due to the MIT, clearly observed for the reference film. The interdiffused film shows no such dramatic changes and retains a Fermi edge, indicating the absence of a band gap, even at low temperature. This reaffirms the evidence of a suppressed MIT and is consistent with the measured low-resistivity state.

The corresponding O K-edge measurements with x-ray polarization $E_{\|}c_R$ are shown in Fig. 4b. The spectrum collected at room temperature for the reference film displays the expected three features for VO_2; the π^* (∼529.5 eV), $d_{\|}^*$ (∼530.5 eV) and σ^* (∼532 eV) bands.[29] The $d_{\|}^*$ band arises from the V 3d_{xy} orbital, which points directly to the next nearest vanadium site. The presence of this feature indicates the splitting of the $d_{\|}$ band due to V-V dimerization in the monoclinic structure. This feature is seen to vanish upon the transition to the metallic rutile (R)-phase VO_2, with evenly spaced vanadium ions.[18,19,29]

The spectra from the interdiffused film show overall similar structure, although there is some additional weight near 531 and 533.5 eV just above the π^* and σ^* bands. This additional weight is associated with π^* and σ^* states resulting from Ti-O bonding (see supplemental material[22]). By taking the difference between the low and high temperature spectra, the temperature-dependent behavior of the $d_{\|}^*$ feature for the interdiffused film is revealed to exhibit a nearly identical lineshape to that of the reference. This indicates that there persists a thermally induced SPT in the interdiffused film, in which direct V-V bonding occurs, resulting in a monoclinic-like phase.

A simplified schematic of the near Fermi level (E_F) electronic states is shown in Fig. 4c. Photoelectron spectroscopy is sensitive to the occupied electronic states while x-ray absorption at the O K-edge measures dipole allowed transitions from the O 1s to unoccupied O 2p

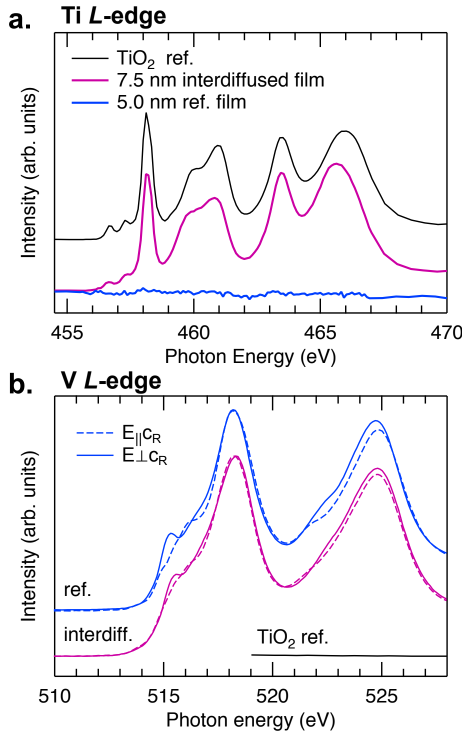

FIG. 3. (a) Ti L-edge XAS of the diffuse 7.5 nm $VO_2/TiO_2(100)$ film as well as a 5 nm film with a sharp interface and a bare TiO_2 substrate for reference and (b) polarization dependent V L-edge XAS of both the interdiffused film and reference film.

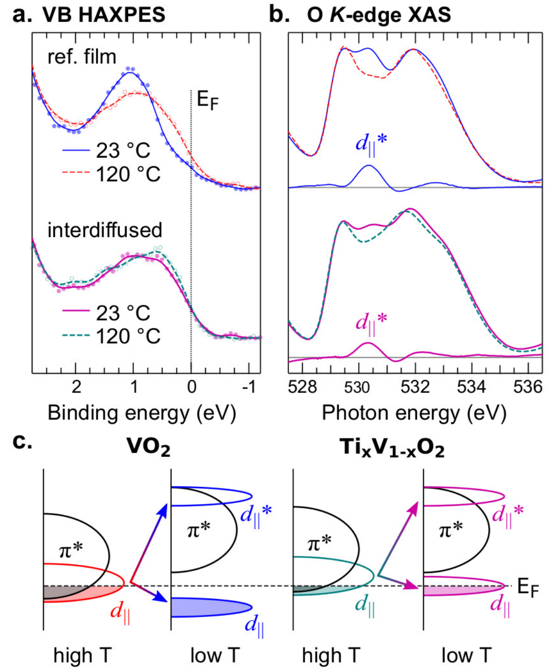

FIG. 4. (a) Valence band HAXPES and (b) O K-edge XAS of a reference VO_2/TiO_2 film measured above and below T_{MIT} as compared to the interdiffused film measured at the same temperatures. The difference spectra highlight the temperature dependence of the $d_{\|}^{*}$ feature. (c) Schematic summary of the near E_F electronic states of VO_2 and $Ti_xV_{1-x}O_2$.

states. In the interdiffused case, the distortion of the lattice at lower temperatures causes the $d_{\|}$ band to split, as it does in pure VO_2, however there is no temperature dependence of the total occupied states. This can be rectified by considering the strict V^{4+} and Ti^{4+} oxidation states. The reduced electron count results in E_F lying within the $d_{\|}$ band and the system remains metallic.

This hole-doping model is tested for both the monoclinic (M1) and rutile (R) structural phases of VO_2 within the DFT+U formalism (see supplemental material[22] for details). V^{4+}/Ti^{4+} cation exchange can be approximated by partially removing the d^1 electron from VO_2 without disturbing the structure. At maximum, one can remove 1 electron/atom, which corresponds to the electronic configuration of Ti^{4+}. DFT+U for undoped R VO_2 yields metallic character while M1 VO_2 displays insulating character with a band gap of 0.3 eV (underestimating the real band gap of 0.7 eV).[30] As R VO_2 is hole doped, it remains metallic except for a very large unphysical hole-concentration $x_h = 1$. The behavior of hole-doped M1 VO_2 is more complicated and undergoes several transitions. At small doping $0 \leq x_h \leq 0.05$ there is an insulator to doped semiconductor transition. As x_h increases, the band gap then gradually decreases. At $0.25 \leq x_h \leq 0.50$ the band gap vanishes and thus a transition to a band-metal takes place. Finally, at maximum (unphysical) doping the M1 phase is insulating again. We estimate from our STEM-EELS analysis that the majority of the interdiffused 7.5 nm film is in a heavily doped range of $Ti_xV_{1-x}O_2$ where $0.25 \leq x \leq 0.75$. Both M1 and R phase VO_2 are expected to be metallic throughout this entire doping range.

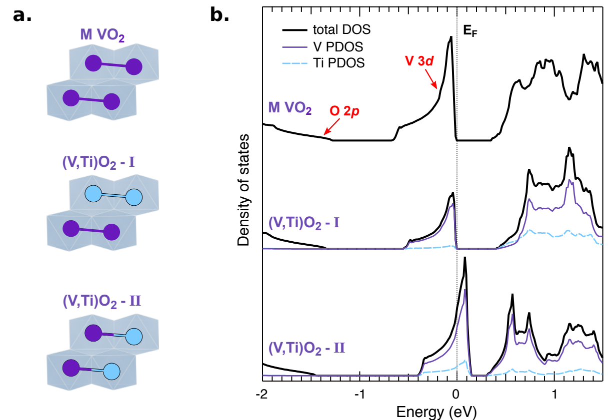

FIG. 5. Projected densities of states from DFT+U for (top) stoichiometric M1-phase VO_2, and M1-phase VO_2 with 50% of the vanadium atoms replaced by titanium atoms forming either (middle) one Ti-Ti and one V-V dimer or (bottom) two V-Ti dimers.

Given this high concentration of Ti observed in the film, a deeper understanding can be gained by considering M1 VO_2 where Ti atoms are explicitly included by replacing half the V atoms. The unit cell of the M1

structure contains four VO_2 formula units and hence two pairs of dimerized metal atoms. To effectively illustrate the different possible atomic arrangements we consider two representative cases illustrated in Fig. 5a. The first case, denoted $(V,Ti)O_2$-I, is a unit cell comprised of one Ti-Ti and one V-V dimer, while the second case, denoted $(V,Ti)O_2$-II, contains two dimerized V-Ti pairs.

The predicted densities of states are shown in Fig. 5b. Only in the $(V,Ti)O_2$-II case do we obtain a metallic DOS, where the Fermi level is well within the V 3*d* band. Hence the model suggests that strict V^{4+} and Ti^{4+} oxidation states without V-Ti dimer formation results in an insulating monoclinic phase. The origin of the metallic behavior in the Ti interdiffused film is therefore a result of a significant concentration of these V-Ti pairs.

We have shown that the high solubility of the Ti ions in VO_2 can result in V^{4+}/Ti^{4+} interfacial cation exchange extending over several nanometers via relatively low temperature annealing. This titanium interdiffusion has considerable effects on the properties of ultra-thin VO_2/TiO_2 films, and can result in an entirely suppressed metal-insulator transition. The presence of V-Ti dimers in interdiffused films is responsible for a metallic-like state at lower temperature. This emphasizes the importance of maintaining abrupt interfaces at the nanometer scale in VO_2/TiO_2 thin films.

Furthermore, we have isolated the charge doping effects of titanium incorporation into ultra-thin VO_2. The replacement of V^{4+} ions with Ti^{4+} ions reduces the V 3*d* electron count, thus tailors the system further away from the Mott criterion. Because of this, the electrons do not become localized into an insulating state even after a Peierls-like distortion. Moreover, the fact that the lattice distortion is still thermodynamically favored at lower temperatures indicates that strong electron correlations are not a necessarily a prerequisite for the rutile to monoclinic structural phase transition of VO_2.

ACKNOWLEDGMENTS

N.F.Q., M.J.W., and L.F.J.P. acknowledge support from the National Science Foundation under DMR 1409912. The HAXPES and XAS measurements presented in the main text were performed at beamlines X24A and U4B, respectively, at the National Synchrotron Light Source. Beamline X24A at the NSLS is supported by the National Institute of Standards and Technology. The NSLS is supported by the U.S. Department of Energy, Office of Science, Office of Basic Energy Sciences, under Contract No. DE-AC02-98CH10886. Additional measurements were performed at beamlines I-09 at Diamond Light Source and 8.0.1 iRIXS of the Advanced Light Source. We thank Diamond Light Source for access to beamline I-09 (SI12546) that contributed to the results presented here. The work at ALS is supported by the 357 Office of Basic Energy Sciences, of the U.S. Department of Energy under Contract No. DE-AC02-05CH11231. The work of H.P. and D.G.S. was supported in part by the Center for Low Energy Systems Technology (LEAST), one of the six SRC STARnet Centers, sponsored by MARCO and DARPA. Electron microscopy by M. E. H., film growth by H.P., and transport measurements by J.M. were supported by the U.S. Department of Energy, Office of Basic Energy Sciences, Division of Materials Sciences and Engineering under Award #DE-SC0002334. Electron microscopy work made use of the Cornell Center for Materials Research Shared Facilities which are supported through the NSF MRSEC program (DMR-1120296). We would like to thank Mick Thomas, John Grazul, and Dr. Earl Kirkland for assistance in the microscope facilities.

---

* lpiper@binghamton.edu

[1] F. J. Morin, Phys. Rev. Lett. **3**, 34 (1959).
[2] J. B. Goodenough, J. Solid State Chem. **3**, 490 (1971).
[3] V. Eyert, Ann. Phys. **11**, 650 (2002).
[4] H. Takagi and H. Y. Hwang, Science **327**, 1601 (2010).
[5] M. Nakano, K. Shibuya, D. Okuyama, T. Hatano, S. Ono, M. Kawasaki, Y. Iwasa, and Y. Tokura, Nature **487**, 459 (2012).
[6] N. Shukla, A. V. Thathachary, A. Agrawal, H. Paik, A. Aziz, D. G. Schlom, S. K. Gupta, R. Engel-Herbert, and S. Datta, Nat. Commun. **6**, 7812 (2015).
[7] Z. Yang, C. Ko, and S. Ramanathan, Annu. Rev. Mater. Res. **41**, 337 (2011).
[8] A. L. Pergament, G. B. Stefanovich, and A. A. Velichko, J. Sel. Top. Nano Electron. Comput. **1**, 24 (2013).
[9] B. Y. Zhou and S. Ramanathan, Proc. IEEE , 1 (2015).
[10] N. F. Quackenbush, H. Paik, M. J. Wahila, S. Sallis, M. E. Holtz, X. Huang, A. Ganose, B. J. Morgan, D. O. Scanlon, Y. Gu, F. Xue, L.-Q. Chen, G. E. Sterbinsky, C. Schlueter, T.-L. Lee, J. C. Woicik, J.-H. Guo, J. D. Brock, D. A. Muller, D. A. Arena, D. G. Schlom, and L. F. J. Piper, Phys. Rev. B **94**, 085105 (2016).
[11] S. Mukherjee, N. F. Quackenbush, H. Paik, C. Schlueter, T.-L. Lee, D. G. Schlom, L. F. J. Piper, and W.-C. Lee, Phys. Rev. B **93**, 241110(R) (2016).
[12] K. Maekawa, M. Takizawa, H. Wadati, T. Yoshida, A. Fujimori, H. Kumigashira, M. Oshima, Y. Muraoka, Y. Nagao, and Z. Hiroi, Phys. Rev. B **76**, 115121(R) (2007).
[13] K. Nagashima, T. Yanagida, H. Tanaka, and T. Kawai, J. Appl. Phys. **101**, 99 (2007).
[14] Y. Muraoka, K. Saeki, R. Eguchi, T. Wakita, M. Hirai, T. Yokoya, and S. Shin, J. Appl. Phys. **109** (2011).
[15] J. W. Tashman, J. H. Lee, H. Paik, J. A. Moyer, R. Misra, J. A. Mundy, T. Spila, T. A. Merz, J. Schubert, D. A. Muller, P. Schiffer, and D. G. Schlom, Appl. Phys. Lett. **104**, 063104 (2013).
[16] B. Zhi, G. Gao, X. Tan, P. Chen, L. Wang, S. Jin, and W. Wu, Mater. Res. Express **1**, 046402 (2014).

[17] H. Paik, J. A. Moyer, T. Spila, J. W. Tashman, J. A. Mundy, E. Freeman, N. Shukla, J. M. Lapano, R. Engel-Herbert, W. Zander, J. Schubert, D. A. Muller, S. Datta, P. Schiffer, and D. G. Schlom, Appl. Phys. Lett. **107**, 163101 (2015).

[18] N. F. Quackenbush, J. W. Tashman, J. A. Mundy, S. Sallis, H. Paik, R. Misra, J. A. Moyer, J. H. Guo, D. A. Fischer, J. C. Woicik, D. A. Muller, D. G. Schlom, and L. F. J. Piper, Nano Lett. **13**, 4857 (2013).

[19] N. F. Quackenbush, H. Paik, J. C. Woicik, D. A. Arena, D. G. Schlom, and L. F. J. Piper, Materials **2**, 5452 (2015).

[20] Y. Yamamoto, K. Nakajima, T. Ohsawa, Y. Matsumoto, and H. Koinuma, Jpn. J. Appl. Phys. **44**, 511 (2005).

[21] M. W. Haverkort, Z. Hu, A. Tanaka, W. Reichelt, S. V. Streltsov, M. A. Korotin, V. I. Anisimov, H. H. Hsieh, H.-J. Lin, C. T. Chen, D. I. Khomskii, and L. H. Tjeng, Phys. Rev. Lett. **95**, 196404 (2005).

[22] See supplemental material [], for details regarding sample growth and characterization, supporting STEM-EELS, HAXPES, and XAS analysis, and details of the DFT+U calculations, which includes Refs.[23–28].

[23] C. Dallera, L. Braicovich, L. Duò, A. Palenzona, G. Panaccione, G. Paolicelli, B. C. C. Cowie, and J. Zegenhagen, Nucl. Instruments Methods Phys. Res. Sect. A Accel. Spectrometers, Detect. Assoc. Equip. **547**, 113 (2005).

[24] G. Kresse and J. Hafner, J. Phys. Condens. Matter **6**, 8245 (1994).

[25] G. Kresse and D. Joubert, Phys. Rev. B **59**, 1758 (1999).

[26] J. P. Perdew, K. Burke, and M. Ernzerhof, Phys. Rev. Lett. **78**, 1396 (1996).

[27] A. I. Liechtenstein, V. I. Anisimov, and J. Zaanen, Phys. Rev. B **52**, 5467 (1995).

[28] J. H. Park, J. M. Coy, T. S. Kasirga, C. Huang, Z. Fei, S. Hunter, and D. H. Cobden, Nature **500**, 431 (2013).

[29] M. Abbate, F. M. F. de Groot, J. C. Fuggle, Y. J. Ma, C. T. Chen, F. Sette, A. Fujimori, Y. Ueda, and K. Kosuge, Phys. Rev. B **43**, 7263 (1991).

[30] S. Shin, S. Suga, M. Taniguchi, M. Fujisawa, H. Kanzaki, A. Fujimori, H. Daimon, Y. Ueda, K. Kosuge, and S. Kachi, Phys. Rev. B **41**, 4993 (1990).